RSC Advances

ROYAL SOCIETY OF CHEMISTRY

www.rsc.org/advances

Development of negatively charged particulate surfaces through a dry plasma-assisted approach

Behnam Akhavan, Karyn Jarvis, Peter Majewski*

[2]*School of Engineering, Mawson Institute, University of South Australia, Mawson Lakes, SA 5095, Australia*

***Corresponding Author:**

Prof. Peter Majewski

School of Engineering

University of South Australia

Mawson Lakes Boulevard

Mawson Lakes, SA, 5095

Australia

Tel: +61 8 83023162

Fax: +61 8 83023380

Email: peter.majewski@unisa.edu.au

ABSTRACT

A dry two-step plasma process is introduced for the fabrication of particulate surfaces showing negative charges over a wide range of pH. Plasma polymerized thiophene (PPT) was initially deposited onto silica particles using an inductively coupled plasma polymerization reactor fitted with a rotating barrel. Sulfur-functionalized particles were further chemically modified through an oxidative air or water plasma treatment. Wide ranges of plasma specific energies (0.06 – 2.4 $kJ.cm^{-3}$) and treatment times (5 – 60 minutes) were employed to manipulate the surface chemistry, hydrophobicity and surface charge of the silica particles. Surface chemistry of the modified silica particles was studied using X-ray photoelectron spectroscopy (XPS) and time of flight secondary ion mass spectroscopy (ToF-SIMS). Changes in hydrophobicity and surface charge of the modified particles were quantified via Washburn capillary rise measurements and electrokinetic analysis, respectively. Plasma treatment of PPT coated particles resulted in homogenous formation of $–SO_x(H)$ functionalities such as sulfonate (SO_3^-), sulfonic acid (SO_3H) and sulfate (SO_4^{2-}) on surfaces. Such changes in surface chemistry significantly decreased the zeta potential and isoelectric point of the particles as well as their degree of hydrophobicity. In comparison to air plasma, water plasma was found to be a better candidate for the treatment of PPT coated particles as it produced surfaces with lower zeta potentials and isoelectric points. Our introduced solvent-free approach is applicable for the modification of almost any other particles regardless of their shape and surface chemistry. Such surface engineered particles could be utilized as protein detectors/adsorbents, solid-state catalysts and heavy metal removal agents.

Key words: plasma treatment, plasma polymerization, surface charge, thiophene, zeta potential

1. INTRODUCTION

Particulate surfaces functionalized with oxidized sulfur groups [$–SO_x(H)$], e.g. sulfonate (SO_3^-), sulfonic acid (SO_3H) and sulfate (SO_4^{2-}), are widely applied as catalysts,[1] protein detectors,[2] chromatographic packing materials[3] and adsorbent agents for water purification.[4] Sulfonate- and/or sulfonic acid-functionalised microspheres have been extensively reported in the literature as favourable protein detectors and adsorbents.[2, 5, 6] In aqueous solutions, $–SO_x(H)$-functionalized particles are highly negatively charged over a wide pH range.[7] Such modified particles have therefore been increasingly applied as electrostatic adsorbents for the removal of cationic contaminants, e.g. heavy metals,[8] ammonium compounds[9] and organic dyes[10]. Silica particles are often employed as low-cost substrates for $–SO_x(H)$ functionalities due to their physico-chemical stability, commercial availability and appropriate surface chemistry.[11]

Oxidised sulfur-functionalized silica particles are conventionally produced through wet-chemistry processes. Two wet-chemistry routes, based on silane chemistry, are typically utilised to introduce oxygen-sulfur moieties onto the surface of silica particles: (i) thiol functionalization of silica particles followed by an oxidation step with hydrogen peroxide;[3, 8, 12, 13] and (ii) amine functionalization of silica particles followed by surface-initiated free radical polymerization.[14] Such routes however result in relatively low densities of $–SO_x(H)$ functionalities in addition to their uneven distribution on the surface.[3] Furthermore, wet-chemistry routes are time consuming, complex and environmentally destructive due to their high rate of waste production.[11, 15] Such methods are also highly substrate-dependent and are therefore restricted to the modification of surfaces with high densities of silanol groups (Si-OH). A pre-cleaning step is thus essential for the removal of surface contamination, which further increases the solvent consumption of the process.[14]

Plasma polymerization is a simple, rapid and solvent-free process,[16] without the issues associated with wet-chemistry methods. The plasma polymerization process is substrate-independent and capable of depositing conformal ultra-thin functionalized polymer films onto a variety of substrates with diverse surface chemistries, shapes and geometries.[17, 18] In this completely dry method, no pre-cleaning step of

the substrate is required and virtually no waste is produced.[19] In a typical plasma polymerization process, a precursor liquid monomer is initially converted to vapour under low pressures, and is then electrically excited into the plasma state. The excited gas consists of active species such as neutrals, electrons, ions and radicals. The recombination of monomer fragments form a nano-thin layer of plasma polymer onto any surface exposed to plasma.[20] In a plasma treatment process, the substrate is physico-chemically modified via a non-polymer forming interaction with an excited gas.[21] In both plasma polymerization and plasma treatment processes, the surface chemistry and thus also the surface charge and hydrophobicity/hydrophilicity of modified substrates are strongly influenced by the plasma process parameters. The most crucial parameters in these processes are plasma input power (W), monomer/treatment gas flow rate (F) and polymerization/treatment time (t).[22] Specific plasma energy, described as input power to flow rate ratio (W/F), denotes the available energy per unit volume of the monomer/treatment gas.[23] The W/F parameter significantly influences the chemical composition of the modified surface, whereas plasma polymerization/treatment time mainly governs the thickness of the polymerized/modified layer.[24]

Functionalized plasma polymer films containing hydrocarbons ($–C_xH_y$),[23] amine ($–NH_2$)[25] or carboxylic acid (–COOH)[26] functional groups are easily obtained via a single-step plasma polymerization of a precursor monomer. The direct deposition of $–SO_x(H)$-functionalized plasma polymer films however is not feasible at ambient temperature due to the low volatility of $–SO_x(H)$-containing monomers, thus hindering the evaporation of the monomer into the plasma chamber.[27] Such an issue has resulted in limited research carried out on the fabrication of $–SO_x(H)$-functionalized plasma polymers. Only a few completely dry plasma-assisted approaches have previously been attempted to deposit $–SO_x(H)$-containing films.[27-29] In these studies, conducted on planar surfaces, sulfur dioxide (SO_2) has been utilised either for copolymerization[28] or post-polymerization[27] treatments. These methods are however still environmentally questionable due to the high toxicity of SO_2.[30] We have recently reported a more efficient and greener approach for the development of oxidised sulfur-containing planar surfaces through a combination of plasma polymerization and an oxidative air/oxygen plasma treatment.[31] The plasma polymerization/treatment of particulate surfaces

is however more complicated than planar surfaces, and thus has not been widely investigated in the literature. As a result of large surface area, the partial exposure of particulate surfaces to plasma causes technological challenges in achieving homogeneously functionalized surfaces. To address this issue, specific designs of plasma polymerization/treatment systems are required. Fluidized bed,[32, 33] particle injection,[34] and rotating[35] reactors have been previously employed for the modification of particles. Our previous investigations have shown effective deposition of hydrocarbon[36, 37] and amine[20, 38] functionalized plasma polymer films onto silica particles using a rotating plasma reactor.

In this investigation, $-SO_x(H)$-functionalized particulate surfaces were produced through a two-step plasma process as schematically illustrated in **Figure 1**. Plasma polymerized thiophene (PPT) films were initially deposited onto silica particles which were subsequently $-SO_x(H)$-functionalized via either air or water plasma treatments. The success of our introduced method in the modification of silica particles surface chemistry has been demonstrated through X-ray photoelectron spectroscopy (XPS) and time of flight secondary ion mass spectroscopy (ToF-SIMS) analyses. Washburn capillary rise measurements and electro kinetic analysis were also implemented to examine the hydrophobicity and surface charge of particles, respectively. These two characteristics of particles are critically important in practical applications and need to be optimized through manipulating the surface chemistry.[7, 39] It has been demonstrated that plasma polymerization of thiophene followed by an air/water oxidative plasma treatment, undertaken in a rotating reactor, is an effective green approach for the fabrication of $-SO_x(H)$-functionalized particles showing negative charges over a wide range of pH.

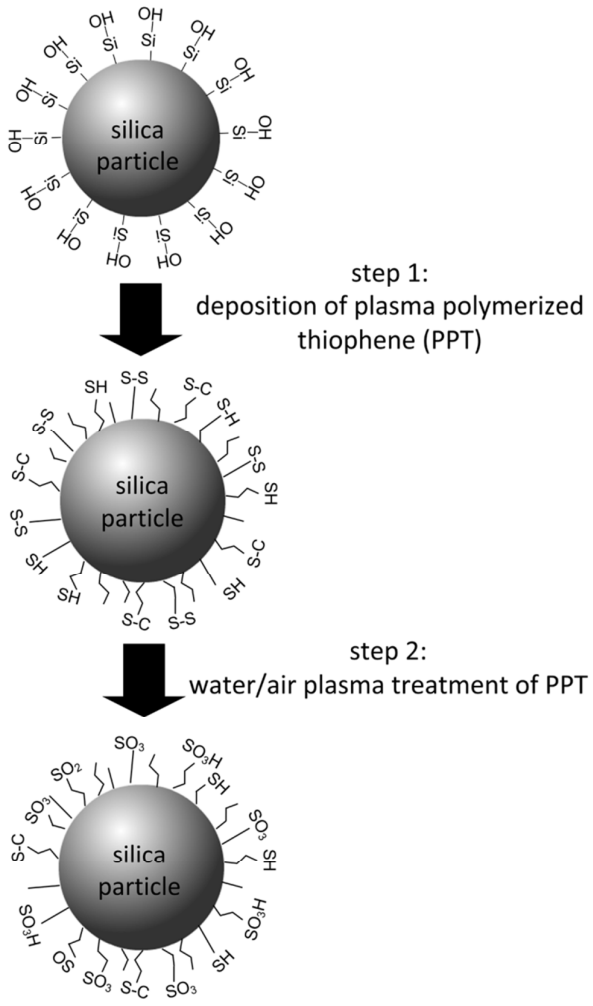

Figure 1. Schematic illustration of the development of $-SO_x(H)$ functionalities on silica particles through a two-step plasma process.

2. EXPERIMENTAL

2.1. Materials

Crystalline silica particles with a size range of 200 – 300 μm and liquid monomer thiophene (C_4H_4S) (purity > 99%) were purchased from Sigma Aldrich (Castle Hill, Australia) and used as received.

2.2. Plasma polymerization

Plasma polymerization of thiophene onto silica particles and plasma treatment of PPT coated particles were conducted employing a custom-built reactor, schematically described previously.[37] The radio frequency (RF) inductively coupled reactor operated with a 13.56 MHz RF generator and a matching network (Coxial Power Systems Ltd.). The reactor was fitted with a rotating chamber and a paddling strip to ensure homogenous modification of particles. A base pressure of approximately 7×10^{-3} mbar was achieved using a rotary vacuum pump after 50 g of silica particles were loaded into the chamber. The liquid monomer thiophene and Milli-Q water were degassed through at least three freeze-thaw cycles, while the chamber was under vacuum. The flow rates of thiophene, water vapour and air were controlled using a needle valve. For each batch of samples, thiophene was initially deposited onto silica particles at an optimum specific energy of 0.08 $kJ.cm^{-3}$ (plasma power = 8 W, thiophene flow rate = 6 sccm) for 30 minutes to ensure the deposition of a sufficiently thick PPT film. Air and water plasma treatment processes were conducted on PPT coated silica particles directly after the deposition, without removal from the chamber. Energy dependent samples were prepared using plasma powers of 2 – 80 W and air or water vapour flow rates of 1 – 10 sccm (standard cubic centimetre) to produce W/F ratios of 0.06 to 2.4 $kJ.cm^{-3}$, while a treatment time of 5 minutes was kept constant. Time-variable samples were produced by varying plasma treatment times from 2 to 60 minutes, as the optimum W/F ratio of 0.3 $kJ.cm^{-3}$ was kept unchanged. A constant rotation speed of 14 rpm was applied for all the polymerization/treatment experiments.

2.3. X-ray photoelectron spectroscopy

XPS analysis was carried out using a SPECS SAGE instrument equipped with a hemispherical analyser (Phoibos 150) and a MCD9 electron detector. The take-off angle was 90^{o} in respect to the sample surface, while a non-monochromatic radiation source (MgKα, hv = 1253.6 eV) was operating at 200 W (10 kV, 20 mA). The survey spectra (0 – 1000 eV) of samples were acquired with a pass

energy of 30 eV and a resolution of 0.5 eV. The high resolution S 2p spectra (0.1 eV) were collected at a pass energy of 20 eV. All the binding energies were calibrated according to the binding energy of aliphatic carbon (285.0 eV) to neutralize the effect of surface charge. Samples were mounted on 1 cm circular pieces of carbon tape, while the circular analysis area was 3 mm in diameter. Quantifications of surface atomic concentrations and curve fittings of S 2p high resolution spectra were conducted using CasaXPS. A linear background, Gaussian (70%) − Lorentzian (30%) line shape and equal full-width at half-maximum (FWHM) were applied. All measurements were carried out no later than a day after deposition or treatment processes.

2.4. Time of flight secondary ion mass spectroscopy

ToF-SIMS data were obtained using a PHI TRIFT V nanoTOF instrument (Physical Electronics Inc., Chanhassen, MN, USA). The $^{79+}$Au pulsed liquid metal primary ion gun (LMIG) was operating at 30 kV under the base pressure of 5×10^{-6} Pa or lower. "Unbunched" Au_1 instrumental configurations were employed to obtain images with optimized spatial resolution. Dual charge neutralization was yielded by an electron flood gun and 10 eV Ar^+ ions. Collection of a representative data set was ensured by recording secondary ions from at least 6 areas of 400 × 400 μm per samples. Spectra analyses and processing of ion map distribution images were undertaken by WincadenceN software (Physical Electronics Inc., Chanhassen, MN, USA).

2.5. Washburn capillary rise measurements

The degree of hydrophobicity of untreated and treated samples was evaluated via Washburn capillary rise method.[40] The employed instrument consisted of a dynamic contact angle meter (DCAT21, Dataphysics) and a Wilhelmy balance, controlled by SCAT software. Before running each measurement, the Washburn tube (6 cm long, 8 mm in diameter) was ultrasonicated in acetone and hexane, rinsed with water and dried for 1 hour at 100 ^{o}C. The tube was packed with 4 g of particles.

While the packed tube was in close contact with water, the mass of adsorbed water into the bed of particles was measured as a function of time. Weight square (m^2) values of penetrated water were plotted against time (t), providing the water contact angle (WCA) of particles according to the Washburn equation:[40]

$$m^2 = \frac{C\rho^2\gamma_{LV}\cos\theta}{\mu} t \qquad (1)$$

Where ρ, μ and γ_{LV} are the density, viscosity and surface tension of the probe liquid, respectively. The capillary constant (C), which mainly depends on the porosity of the packed bed, was defined using n-hexane as a total wetting liquid.

2.6. Electrokinetic analysis

Zeta potentials of untreated and treated PPT coated particles were measured using an Anton Paar Electro Kinetic Analyser equipped with a remote titration device. A powder cell (1 cm in diameter and 1 cm long) was packed with particles and placed in the middle of a cylindrical cell with Ag/AgCl electrodes. The pH of 1×10^{-3} M KCl solution was adjusted to approximately 10 using 0.1 M KOH and was then utilised as electrolyte. The pH of the electrolyte was lowered by approximately 0.5 unit steps as appropriate volumes of 0.1 M HCl were injected into the electrolyte container by the remote titration device. Zeta potential measurements were taken at each pH value while the electrolyte was pumped into the cell from right to left and left to right. The measurements were repeated for three times, producing 6 values for each data point. The values were averaged and reported as the zeta potential at a specific pH.

3. RESULTS AND DISCUSSION

3.1. Deposition of PPT films onto silica particles

$-SO_x(H)$ functionalization of silica particles was carried out through two steps: (i) plasma polymerization of thiophene onto silica particles and (ii) oxidative plasma treatment of sulfur-functionalized silica particles. Our preliminary studies showed that plasma specific energy of 0.08 $kJ.cm^{-3}$ and deposition time of 30 minutes produced optimized PPT coatings onto silica particles, where the maximum density of sulfur-containing functionalities was achieved. **Figure 2** shows the XPS survey spectra of uncoated and PPT coated silica particles. The silica particles showed silicon and oxygen signals with atomic concentrations of 29.2% and 54.6%, respectively. Silica particles were applied as substrates without any pre-cleaning process and thus showed 16.2% of adventitious carbon on the surface. It is observed that by the deposition of a PPT film, a sulfur (S 2p) peak with an atomic concentration of 18% emerges at the binding energy (BE) of ~ 164 eV, while no silicon signals contribute to the spectra. A significant increase in the carbon atomic concentration from 16.2% to 75.2% and a significant decrease of oxygen atomic concentration from 54.6% to 6.8% is also observed upon plasma polymerization of PPT film onto silica particles. The atomic concentrations of sulfur and carbon increase as plasma polymer films from the thiophene monomer are deposited onto the particles. The decrease of oxygen concentration and the absence of a silicon peak denote the presence of a sufficiently thick PPT layer onto silica particles which has obscured the underlying substrate signals. The sampling depth of XPS analysis using MgKα source and take-off angle of 90^o is 8 – 10 nm.[20] It can be therefore estimated that the deposited PPT layer is at least 8 nm thick. Although no oxygen is present in the chemical structure of thiophene (C_4H_4S), it still contributes for approximately 7% in the XPS survey spectra of PPT coated particles. The detected oxygen cannot result from the silica substrates as no silicon is observed in the spectra, demonstrating that the substrate is completely obscured by the PPT film. The oxygen can however originate from three possible sources: post-deposition oxidation, air or water contamination in the plasma chamber, and/or highly oxygenated substrate.[41-43]

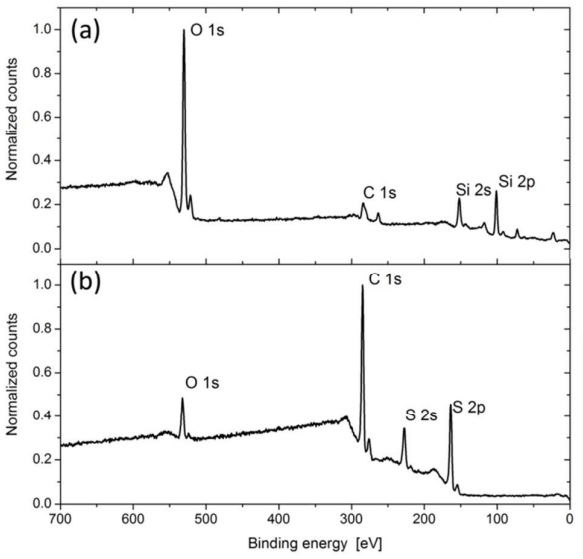

Figure 2. XPS survey spectra of (a) uncoated and (b) PPT coated silica particles. (Plasma specific energy = 0.08 kJ.cm^{-3}, polymerization time = 30 minutes)

ToF-SIMS is a highly surface sensitive spectroscopy technique (analysis depth = 1 – 2 nm) providing valuable information on the molecular structure of a surface.[44] Spatial distribution maps of functional groups can also be obtained via this technique. Such distribution maps are of particular interest in surface engineering of particulate surfaces as they reveal the homogeneity of modified particles. The normalised negative SIMS counts of uncoated and PPT coated silica particles are shown in **Figure 3a**. As observed, plasma polymerization of thiophene results in a decrease of OH^- and Si^- counts and an increase in CH^- and sulfur-containing species (S^-, SH^-, SO^- and SO_3^-). The changes in surface chemistry were expected due to the deposition of thiophene which adds carbon and sulfur containing species on the surface, and masks the oxygen and silicon signals originating from the silica surface. It is also observed that sulfur-oxygen species do not significantly contribute to the overall counts, while sulfur atoms in a neutral environment (S^- and SH^-) are predominant. The distribution maps of SH^- counts for uncoated and PPT coated silica particles are displayed in **Figure 3b**. From these images, not only the high density of SH^- counts is clearly observed, but also their homogeneous distribution on the surface is apparent. These results further validate the XPS data (**Figure 2**) and confirm the successful deposition of sulfur-rich films onto silica particles.

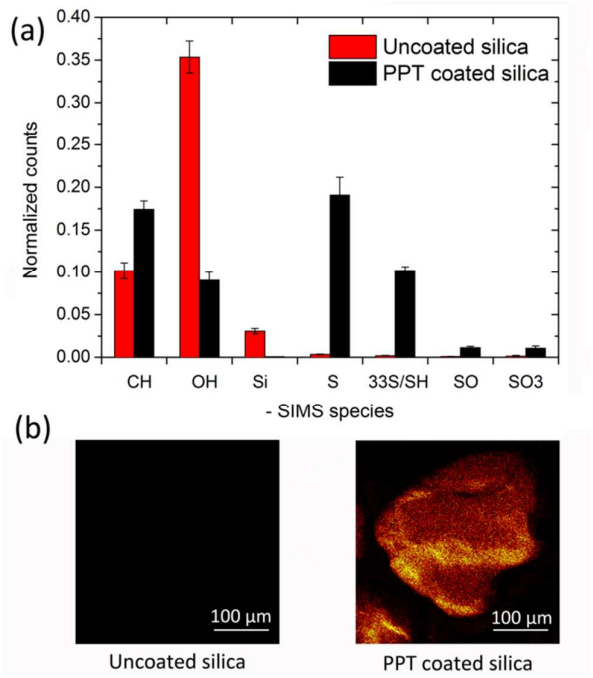

Figure 3. (a) Average normalized -SIMS counts from ToF-SIMS for uncoated and PPT coated silica particles (95% confidence intervals, N ≥ 6), (b) SH^- ion distribution maps from ToF-SIMS for uncoated and PPT coated silica particles. (Plasma specific energy = 0.08 $kJ.cm^{-3}$, polymerization time = 30 minutes)

3.2. Oxidation of PPT coated silica particles through air/water plasma

3.2.1. Influence of plasma specific energy

For the development of $–SO_x(H)$ functionalities onto particulate surfaces, PPT coated particles were treated via air and water plasmas. In our recent study conducted on the modification of PPT coated planar surfaces, it was observed that both air and oxygen plasmas result in a substantial increase of sulfur-oxygen moieties on the surface. Oxygen plasma however showed a significantly higher etching rate in comparison to air plasma.[31] To minimize the rate of etching and achieving a milder oxidation process, water plasma was applied instead of oxygen plasma and its oxidation/etching behaviour was compared with air plasma. Plasma oxidation of polymer surfaces is however always accompanied by a degree of ablation process.[27] The predominance of one of these two processes can be controlled through carefully adjusting the processing parameters such as plasma input power and flow rate of the oxidative gas. Plasma input power (W) to gas flow rate (F) ratio (W/F), also referred to as the plasma

specific energy,[45] represents the available energy per unit volume of the oxidative gas. To study the influence of this parameter in air/water plasma treatment of PPT coated particles, the W/F ratio was varied from 0.06 to 2.4 kJ.cm^{-3}, while the treatment time of 5 minutes was kept constant. The changes of surface chemistry as a function of plasma treatment W/F ratio are plotted in **Figure 4**. The sulfur atomic concentration significantly reduces upon either air or water plasma treatment, while increasing the plasma specific energy up to approximately 0.75 kJ.cm^{-3} increases the atomic concentration of oxygen. The increase in oxygen atomic concentration from 7.0% for untreated PPT coated particle to ~17% for particles treated at W/F = 0.3 kJ.cm^{-3}, with either air or water plasma, suggests the successful incorporation of oxygen atoms in the structure of PPT coatings. The formation of oxygen-containing groups is mainly governed by the generation of O and OH radicals in air and water plasma, respectively.[16, 46] Such radicals are highly reactive and participate in the oxidation of sulfur-containing functionalities through an activation/oxidation mechanism. According to this theory, large concentrations of surface-bond radicals are initially generated on the surface of PPT coated particles as a result of surface bombardment. The generated unstable sites further react with oxygen-containing species present in the plasma environment, and produce stable oxygen-containing moieties.[47, 48] As the W/F ratio increases, more energy per unit volume of air or water vapour becomes available in the plasma state; therefore more reactive radicals are regenerated, resulting in a higher rate of surface oxidation. The plasma treatment of PPT coated particles at relatively high W/F ratios of greater than 1.2 kJ.cm^{-3} however results in a noticeable decrease of oxygen and increase of sulfur atomic concentrations. The oxygen atomic concentration, for example, decreases from its maximum value of 19.3% at W/F = 0.45 kJ.cm^{-3} to 13.9% at W/F = 2.4 kJ.cm^{-3} for air plasma treated samples. According to these changes in surface chemistry, it may be assumed that the oxidation rate of PPT coated particles reduces at high specific energies, where the PPT layer is ablated off the surface before the formation of sulfur-oxygen moieties.

To further elucidate the oxidation/ablation theory, the changes in the atomic concentration of silicon should be taken into account. As discussed in section 3.1, no silicon is observed for untreated PPT coated particles, indicating film thicknesses of at least 8 nm. For particles treated with air and water

plasmas at W/F ratios less than 0.45 and 1.2 kJ.cm^{-3} respectively, still no contribution of silicon is observed; whereas upon undertaking plasma treatments at greater specific energies, silicon signals are detected. The contribution of silicon in XPS survey spectra indicates that the thickness of PPT coatings is reduced to less than 8 nm, the sampling depth of XPS. Such variations in silicon atomic concentration versus W/F ratio implies that the ablation process is not significant at low specific energies, whereas it becomes more pronounced at higher W/F values. The ablation processes is directly related to the kinetic energy of ions and radicals attacking the surface.[49] It can be therefore suggested that at higher W/F ratios, where more energy is available per unit volume of air or water vapour, the PPT layer is ablated at higher rates due to the presence of ions and radicals with higher kinetic energies. For the water plasma treated samples, silicon signals start to contribute in XPS data at a lower specific energy value (W/F =0.45 kJ.cm^{-3}) in comparison to the air plasma treated samples (W/F = 1.2 kJ.cm^{-3}). Such a marked difference can be attributed to the superior ablation potential of water plasma compared to air plasma, resulting from the higher concentration of reactive OH radicals in the plasma environment.[16] According to the changes of surface chemistry, it can be concluded that the oxidation process is prevalent at lower W/F ratios, whereas at higher specific energies the ablation process becomes predominant.

The air plasma treatment of PPT coated particles at W/F ratios greater than 0.06 kJ.cm^{-3} yields incorporation of nitrogen atoms into the PPT layer, reaching a maximum of 3.6% at W/F = 1.8 kJ.cm^{-3}. The incorporation of nitrogen atoms within the PPT layer is however less significant than that of oxygen atoms. This behaviour can be correlated to the significantly smaller dissociation energy of O_2 (498 kJ·mol^{-1}) compared to N_2 (945 kJ·mol^{-1}).[50] Such a difference in binding energy results in fewer numbers of electrons that, at a constant W/F ratio, obtain sufficient energies to split nitrogen bonds. A high number of intact N_2 molecules are therefore pumped out of the plasma chamber without any interaction with the PPT layer. The absence of nitrogen atoms in the surface chemistry of PPT coated particles treated at very low W/F ratio of 0.06 kJ.cm^{-3} further supports this theory. As observed from **Figure 4**, the increase in oxygen atomic concentration is also accompanied by a slight decrease in carbon. The decrease of carbon atomic concentration is however more significant for air plasma

treated samples compared to water plasma. The lower atomic concentrations of carbon observed for air plasma treated samples appear to be associated with the contribution of nitrogen atoms to the overall surface chemistry, thus lowering the relative contribution of carbon atoms. According to these results, it is suggested that relatively low specific energies in a range of 0.15 to 0.3 kJ.cm^{-3} yield the most efficient oxidation of PPT coated particles, where the maximum concentration of oxygen atoms is achieved on the surface and the influence of the ablation process is minimal.

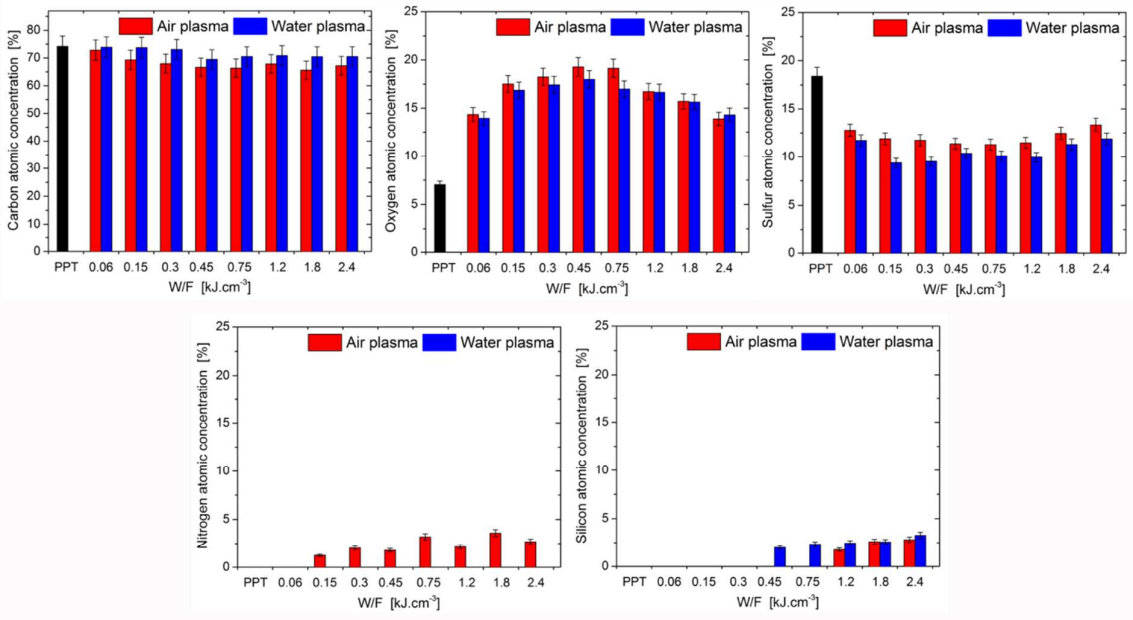

Figure 4. XPS survey elemental compositions of PPT coated silica particles treated with air/water plasma as a function of plasma specific energy. (Plasma treatment time = 5 minutes)

3.2.2. Influence of plasma treatment time

Plasma treatments conducted at low plasma specific energies yielded maximum incorporation of oxygen atoms into the treated PPT layers. Plasma treatment time however also plays an important role in tuning the surface properties of PPT coated particles by controlling the depth of the modified layer. To evaluate the influence of plasma treatment time on the surface properties of the PPT coated particles, air and water plasma treatments were conducted for durations of 5 to 60 minutes at a constant W/F ratio of 0.15 kJ.cm^{-3}. While plasma specific energies of 0.15 and 0.3 kJ.cm^{-3} resulted in

maximum oxidation of PPT films, the W/F ratio of 0.15 kJ.cm^{-3} was applied for time-dependent studies to minimize the influence of ablation process. The XPS elemental compositions of PPT coated particles treated with air/water plasma are plotted as a function of treatment time and shown in **Figure 5**. Upon treatment of PPT coated particles via either air or water plasma, the atomic concentration of oxygen increased, while that of sulfur and carbon decreased. These changes are accompanied by a slight increase of nitrogen for air plasma and a significant increase of silicon atomic concentration for both air and oxygen plasmas. These changes in surface chemistry are once again associated with the oxidation and ablation processes. As more oxygen atoms are incorporated into the structure of PPT layer, the atomic concentrations of carbon and sulfur decrease due to their less contribution to the overall spectra. The atomic concentration of oxygen increased from 7% for the untreated PPT coated particles to 19.0% and 20.2% for the samples treated for 10 minutes with air and oxygen plasma, respectively. Such an increase in oxygen atomic concentration suggests significant incorporation of oxygen atoms into the PPT layer. From **Figure 5** it is also evident that by increasing the plasma treatment time over 10 and 20 minutes, for air and water plasma respectively, the silicon signals begin contributing to the surface chemistry, indicating film thicknesses of less than 8 nm. It can be therefore suggested that the oxygen signals for these samples originate from both the modified PPT layer and the silica substrate beneath. The increase of silicon atomic concentrations with plasma treatment time indicates a continuing reduction of the PPT layer thickness due to the previously discussed ablation process. The ablation of PPT layers is also likely to take place at shorter treatment times, but it cannot be determined via XPS as the thicknesses are greater than the sampling depth of this technique. For treatment times of 45 and 60 minutes, the observed silicon and oxygen atomic concentrations are significantly higher for water plasma compared to air plasma, whereas that of sulfur and carbon are markedly lower. Such behaviour indicates a higher contribution of the silica substrates to the overall XPS signals, which agrees with the higher ablation rate of water plasma in comparison to air as observed for energy-dependent samples.

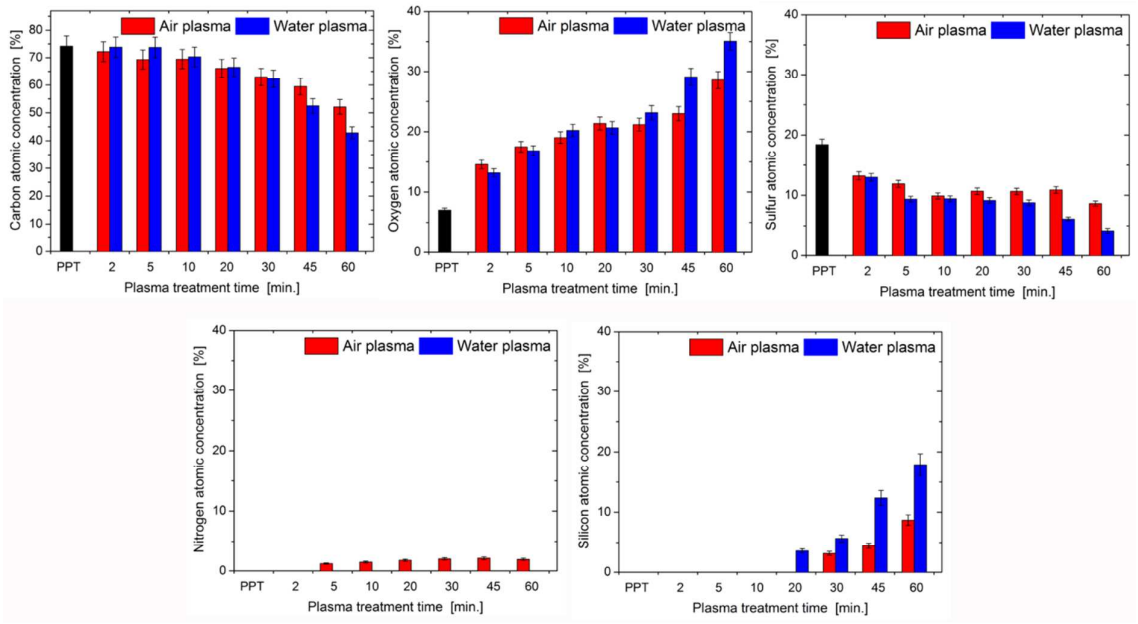

Figure 5. XPS survey elemental compositions of PPT coated silica particles treated with air/water plasma as a function of plasma treatment time. (Plasma specific energy = 0.15 kJ.cm^{-3})

To evaluate the development of –SO_x(H)-containing moieties onto the silica particles, the S 2p high resolution spectra of PPT coated particles treated for different times are curve fitted and displayed in **Figure 6**. The S 2p peak exhibits a doublet structure resulting from the spin-orbit coupling of S $2p_{1/2}$ and S $2p_{3/2}$ with a splitting binding energy (BE) of 1.2 eV.[51] The photoionization cross-section of S $2p_{1/2}$ is half of S $2p_{3/2}$ and therefore the area ratio of S $2p_{1/2}$ to S $2p_{3/2}$ was set to 50%.[27] According to the literature,[27, 52, 53] S 2p high resolution spectra may consist of sulfur-containing groups in neutral environments (S-H, S-C and S-S), oxidised sulfur groups at low oxidation states (S-O and SO_2) and oxidised sulfur groups at high oxidation states (SO_3H, SO_3^-, and SO_4^{2-}). The binding energies associated with these three categories of sulfur-containing moieties are 163 – 165, 165 – 167 and 165 – 167 eV, respectively. The sulfur-oxygen moieties cannot however be separately distinguished in curve fitting studies as the differences of their binding energies are too discreet.[52, 54] The S 2p spectrum of untreated PPT coated particles predominately consists of sulfur-containing groups in a neutral environment (BE = 163 – 165 eV). By increasing the air/water plasma treatment time, the evolution of sulfur-oxygen groups at higher binding energies (> 166 eV) is apparent. In order to quantify the formation of –SO_x(H) functionalities onto the surface of PPT coated particles, atomic

concentrations of different sulfur-containing moieties are determined from peak fitted spectra and are listed in **Table 1**. By increasing the plasma treatment time for both air and water plasmas, the atomic concentrations of sulfur atoms in the neutral state (S-H, S-S, S-C) decrease and that of oxidized sulfur groups increase. Approximately 40% and 49% of sulfur atoms present on the surface of PPT coated particles are oxidized into oxygen-containing moieties after 60 minutes of treatment via air and water plasma, respectively. Water and air plasma treatments result in approximately equal concentrations of SO_3^-, SO_3H and SO_4^{2-} functionalities up to a treatment time of 30 minutes. By further increasing the treatment time, relatively higher concentrations of these functionalities are observed for water plasma treated samples compared to air plasma. Such a difference can be attributed to a greater influence of underlying oxygen signals on the surface chemistry, resulting from the higher ablation rate of water plasma, and therefore thinner PPT films concealing the substrate. From **Table 1**, it is also observed that the concentrations of SO/SO_2 groups do not significantly change against plasma treatment time; whereas that of sulfur groups at high oxidation states, such as sulfonic acid (SO_3H), sulfonate (SO_3^-) and sulfate (SO_4^{2-}), significantly increase. The lower concentration of SO and SO_2 functionalities in comparison to SO_3^-, SO_3H and SO_4^{2-} groups can be attributed to the lower stability of partially oxidized groups, resulting in their further oxidation to more stable states. Air plasma treatment of PPT coated particles produced significantly lower concentrations of –SOx(H) functionalities than was observed for planar surfaces in our recent study.[31] The greater surface area of particulate surfaces in comparison to planar surfaces appears to be responsible for the lower concentration of sulfur-oxygen moieties achieved on silica particles. Higher surface areas result in lower exposure of deposited sulfur-containing groups to oxidative plasma, thus also decreasing the rate of activation/oxidation mechanism. S 2p high resolution curve fitting results, which are in agreement with the rise of oxygen atomic concentrations as a function of plasma treatment time (**Figure 5**), indicate that the neutral sulfur moieties are successfully oxidised into high oxidation states during the oxidative plasma treatment.

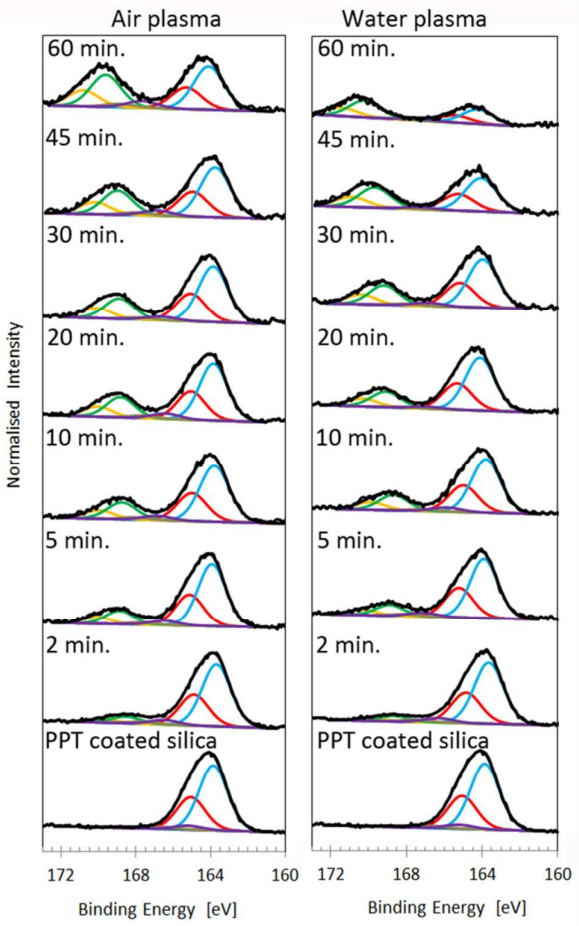

Figure 6. XPS S 2p curve fitted spectra of PPT coated silica particles treated with air/water plasma as a function of treatment time. (Plasma specific energy = 0.15 kJ.cm^{-3})

Table 1. XPS atomic concentrations of curve fitted S 2p components for PPT coated silica particles treated with air/water plasma.

Oxidation time [min.]	XPS atomic concentration of Sulfur-containing moieties [%]		
	S-H, S-C S-S	SO,SO_2	SO_3^-, SO_3H SO_4^{2-}
		PPT	
0	92.9	5.6	1.5
		Air plasma	
2	84.5	6.4	9.1
5	77.5	5.7	16.8
10	72.4	5.8	21.8
20	68.8	6.6	24.6
30	69.6	4.7	25.7
45	62.6	6.9	30.5
60	52.5	8.4	39.1
		Water plasma	
2	86	6.3	7.7
5	79.9	5.5	14.6
10	73.3	5.7	21
20	74.9	3	22.1
30	67.6	4.9	27.5
45	59.5	4.1	36.4
60	43.8	5	51.2

The sulfur-oxygen moieties obtained on the surface of treated particles were further identified via ToF-SIMS analysis. The normalised negative SIMS counts of untreated and treated PPT coated particles are shown in **Figure 7**. Both air and water plasma treatments of PPT coated particles result in a decrease in thiol and sulfur counts and an increase in oxygen and all the oxygen-sulfur counts such as sulfonate, sulfonic acid and sulfate. Such data, which identify the individual sulfur-containing groups, are of particular importance as these groups could not be separately identified through XPS analysis. The maximum increase of $–SO_x(H)$ functionalities is observed for the initial treatment times of 2 and 10 minutes for air and water plasma treated samples, respectively. Such behaviour is once again attributed to the higher oxidation rate of water plasma compared to air plasma. These results however appear to be inconsistent with XPS data which showed continuous changes of surface chemistry within the whole range of treatment times. Such a discrepancy is associated with the distinctly higher surface sensitivity of ToF-SIMS (sampling depth = 1 – 2 nm) compared to that of XPS (sampling depth = 8 – 10 nm).[20, 44] From **Figure 7,** it is also observed that no noticeable silicon counts were collected for the samples treated for shorter than 60 and 30 minutes with air and water plasmas, respectively. The high number of Si^- counts collected for samples treated for 60 minutes, which is also accompanied by a noticeable decrease of sulfur-containing counts, implies PPT thicknesses of less than 2 nm. This behaviour, consistent with XPS results, is once again explained by the ablation of PPT films which occurred during such a prolonged plasma treatment process. The ToF-SIMS data indicate the successful formation of $–SO_x(H)$ functionalities onto the surface of silica particles and further validate the results obtained from XPS survey spectra (**Figure 5**) and S 2p high resolution curve fitting studies (**Figure 7** and **Table 1**).

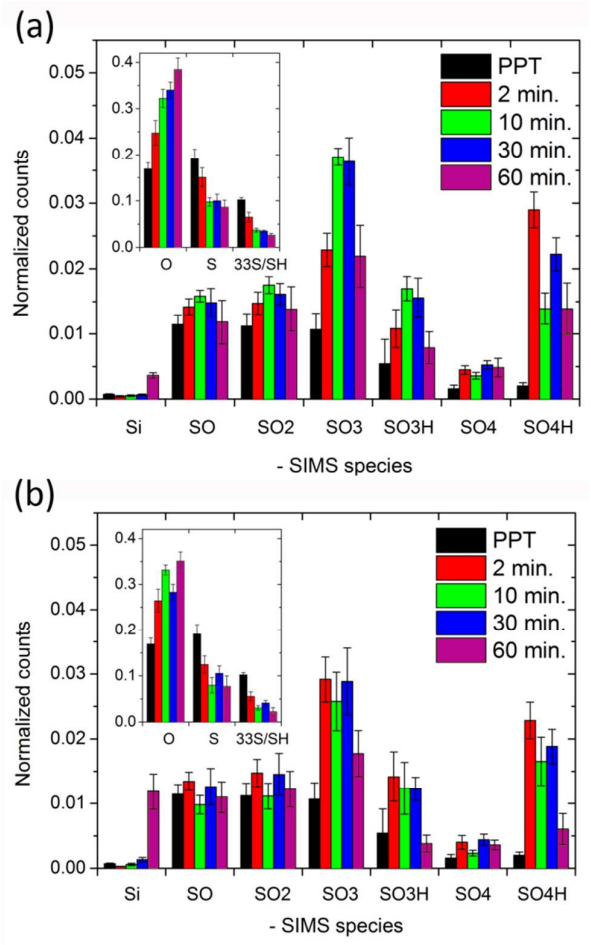

Figure 7. Average normalized negative SIMS counts from ToF-SIMS for PPT coated silica particles treated with (a) air and (b) water plasmas. (95% confidence intervals, $N \geq 6$; plasma specific energy = 0.15 kJ.cm^{-3})

Sulfur-oxygen functional groups need to be evenly distributed onto particulate surfaces for their efficient performance in practical applications such as water purification and protein adsorption. The effectiveness of our introduced approach in the development of homogenously distributed –SO_x(H) functional groups onto silica particles was evaluated via ToF-SIMS imaging. The sum of SO_3^-, SO_3H^- and SO_4H^- ions distribution maps for different air and water plasma treatment times are shown in **Figure 8**. The increase of $SO_x(H)^-$ counts upon air or water plasma treatment of PPT particles is apparent in these images. It is also observed that SO_x(H) functionalities are homogeneously generated onto the silica particles even for a treatment time of as low as 2 minutes. The continuous increase of –

$SO_x(H)$ functionalities as a function of treatment time observed from XPS data could potentially result from the increase of the depth of the modified layer and/or the lateral increase of modified areas. The later phenomenon is valid if only $–SO_x(H)$ functionalities are generated in a patchy-like manner onto the surfaces. The observed homogeneous distribution of $SO_x(H)^-$ counts onto silica particles however proves that the increase of XPS sulfur-oxygen functionalities versus treatment time is mainly due to the increase of the depth of the modified layer. The comparison of $SO_x(H)^-$ ion distribution maps of treated samples for 60 minutes to those treated for 10 minutes highlights the significant decrease of $SO_x(H)^-$ density associated with the ablation process. According to the findings of surface chemistry analyses, it can be concluded that our developed two-step plasma polymerization/treatment process is a promising dry approach for the development of $SO_x(H)$-functionalized particulate surfaces.

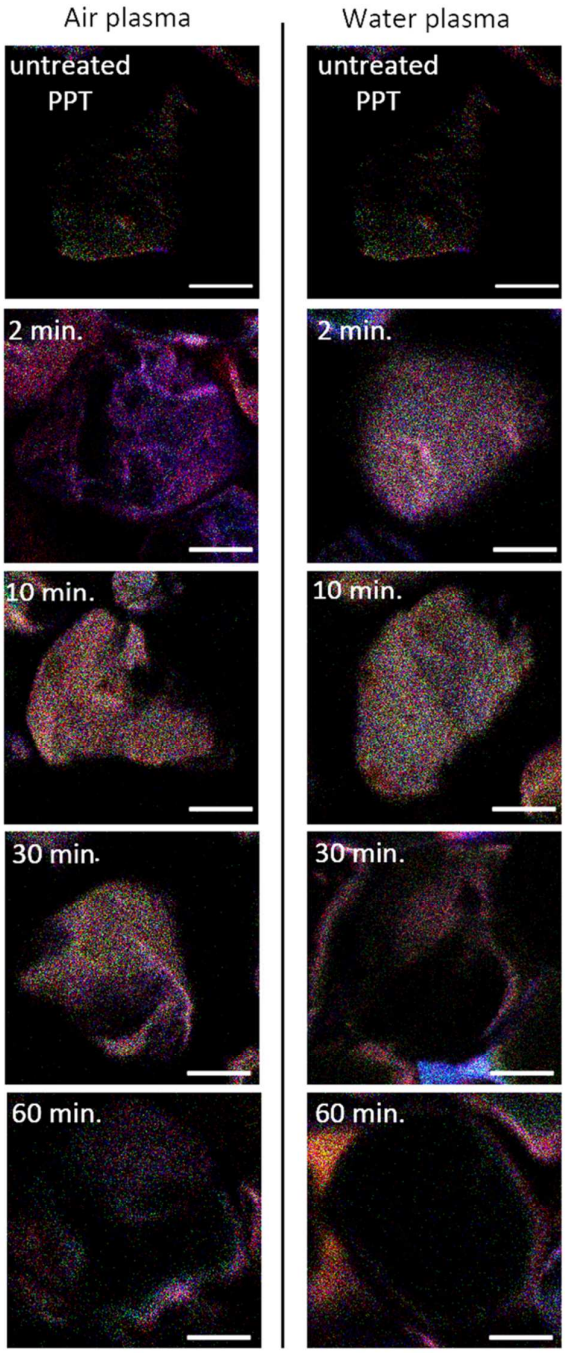

Figure 8. Sum of SO_3^-, SO_3H^- and SO_4H^- ions distribution maps from ToF-SIMS for PPT coated silica particles treated with air and water plasma. Scale bar = 100 µm. (Plasma specific energy = 0.15 $kJ.cm^{-3}$)

3.3. Surface hydrophobicity of –SO_x(H)-functionalized silica particles

The hydrophobicity of functionalized particles plays a key role in solid-liquid interactions involved in practical applications such as adsorption/detection of proteins and removal of cationic pollutants. More hydrophobic particles show lower affinity for polar molecules and also demonstrate lower dispersion/higher aggregation in polar media.[16, 37, 39] The hydrophobicity of untreated and treated PPT coated particles was determined by Washburn capillary rise experiments, which assessed the sorption kinetics of water into the packed bed of particles. The mass of adsorbed water into the packed bed of PPT coated particles treated with air/water plasma are plotted as a function of time after contact and shown in **Figure 9**. It is apparent that virtually no water was adsorbed into the bed of PPT coated particles, indicating a water contact angle (WCA) of greater than 90°. The slight increase in the mass of adsorbed water for untreated PPT coated particles, in comparison to the empty tube, is attributed to the adsorption of water into the paper filter placed at the bottom of the Washburn cell. Such a highly hydrophobic character is attributed to the presence of non-polar hydrocarbon (-CxHy) functionalities[23] and thiol (-SH) groups[55] in the structure of untreated PPT layers. It is observed that upon only 5 minutes of air/water plasma treatment, the adsorption rate of water increases; giving WCAs of 81.4° and 84.8° for air and water plasma, respectively. The decrease of WCA, i.e. the increase in surface hydrophilicity, is explained by the formation of polar oxygen-containing functionalities such as sulfonate and sulfonic acid groups, as suggested by XPS and ToF-SIMS results. Samples treated for 10 minutes with air and water plasma show WCAs as low as 37.3° and 31.8°, respectively. The WCA's of treated particles remained virtually unchanged by further increasing the plasma treatment time. Such a significant increase of surface hydrophilicity observed in just 10 minutes of plasma treatment is attributed to the high surface sensitivity of water contact angle measurement which only interacts with the top most 0.5 nm of a surface.[19, 56] The observed hydrophilic character of these samples denotes surfaces sufficiently functionalized by polar groups. These results are consistent with surface chemistry findings and further corroborate the formation of oxygen-containing groups including oxidised sulfur functionalities on the surface of PPT coated silica particles.

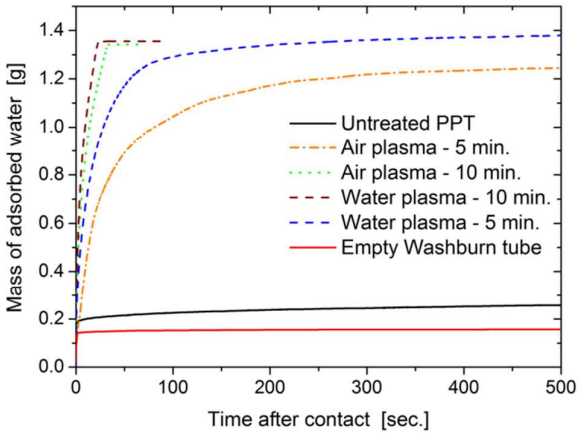

Figure 9. Mass of adsorbed water into the packed bed of PPT coated particles treated with air/water plasma as a function of time after contact. (Plasma specific energy = 0.15 kJ.cm^{-3})

3.3. Zeta potential of –SO$_x$(H)-functionalized silica particles

The surface charge of modified PPT coated particles is of particular importance for adsorption applications such as heavy metal removal.[57] It is ideally required that particles applied for such applications show the highest negative charge density over the greatest pH range.[7] The surface charge is typically evaluated by the magnitude of zeta potential which refers to the electrical potential at the shear plane.[58, 59] Zeta potential measurements are strongly pH-dependent as the dissociation of functional groups strongly varies with pH.[59] To evaluate the influence of air/water plasma treatment on the electrokinetic behaviour of silica particles, the zeta potential measurements were conducted over a pH range of 3 - 10 at a constant ionic strength. The zeta potential changes of untreated and air/water plasma treated PPT coated particles are plotted as a function of pH and shown in **Figure 10**. Increasing the pH value decreases the zeta potentials of particles for all samples. The zeta potential of PPT coated particles is zero at pH = 4.3, which is identified as the isoelectric point (IEP).[60] At pH values greater than IEP, the surfaces possess a net negative charge; while at pH values less than IEP, surfaces carry a net positive charge. The zeta potential of PPT coated particles over pH values greater than 4.3 is due to the deprotonation of acidic sulfur-containing groups such as thiol (RSH → RS$^-$ +

H^+).[7] The positive zeta potentials observed at pH values smaller than 4.3 suggest the protonation of sulfur-containing groups.

It is observed that water plasma treatment of PPT coated particles significantly reduces the zeta potential and IEP. The most positive zeta potential of -34.8 mV (at pH = 10) for untreated PPT coated particles decreases to -66.7 mV (at pH = 10) for PPT coated particles treated with water plasma for 5 minutes. Such a significant decrease in zeta potential is accompanied by a noticeable decrease of IEP from 4.3 to below 3.5. These changes are due to the dissociation of introduced strong acidic groups such as SO_3H ($SO_3H + H_2O \rightarrow SO_3^- + H_3O^+$) and presence of negatively charged moieties such as sulfonate (SO_3^-) and sulfate (SO_4^{2-}), as evident by XPS and ToF-SIMS results. Sulfate groups, for example, are always fully deprotonated in aqueous conditions.[61] The decrease of zeta potential by the increase of pH is attributed to the higher rate of deprotonation reactions at higher pH values.

From **Figure 10**, it is also observed that PPT coated particles treated for 5 minutes with air plasma exhibit significantly lower zeta potentials, in comparison to particles treated with water plasma for the same duration. The IEP of air plasma treated sample is also recorded at the significantly higher pH value of 3.6 compared to that of water plasma treated sample (IEP < 3.5). A maximum zeta potential difference of approximately 25 mV is observed for these two samples at pH ≈ 9. These changes appear to be linked to the incorporation of nitrogen atoms to the surface, as shown by XPS data (**Figure 5**). According to this data, air plasma treated particles contain approximately 2% of nitrogen which may play a considerable role in reducing the negative zeta potential of particles. The influence of nitrogen-containing species on the zeta potential results from their lower affinity in deprotonation at high pH values in comparison to sulfur-containing moieties.[7] The protonation of these species at low pH values produces positively charged groups, such as NH_3^+, which evidently reduce the negative zeta potential.[20] By increasing the treatment time to 60 minutes, zeta potentials and IEP increase for both air and water plasma. Such changes were expected due to the influence of the ablation process, resulting in lower concentration of $–SO_x(H)$ functionalities on the surface. The electrokinetic analysis results confirm that plasma polymerization of thiophene followed by air/water plasma treatment results in highly negatively charged $–SO_x(H)$-functionalized particulate surfaces. It can also be

concluded that water plasma treatment of PPT coated particles is preferred over air plasma treatment, as it produces surfaces with lower zeta potentials and IEPs.

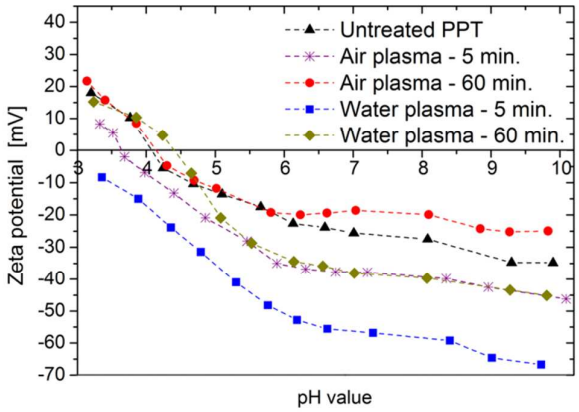

Figure 10. Zeta potential of PPT coated particles treated with air/water plasma as a function of pH. (Plasma specific energy = 0.15 kJ.cm^{-3})

4. CONCLUSIONS

A completely dry method has been introduced for the development of oxidized sulfur-terminated particulate surfaces. Particulate surfaces were successfully developed via plasma polymerization of thiophene followed by air/water plasma treatment process. Oxidative plasma treatments of PPT coated silica particles resulted in significant changes of surface chemistry which consequently influenced the zeta potential and hydrophobicity of modified particles. XPS and ToF-SIMS results confirmed the formation of oxidised sulfur functional groups, such as sulfonate, sulfonic acid and sulfate on the surface of silica particles. Such functionalities resulted in a significant decrease in zeta potential and a noticeable shift of the isoelectric point to lower pH values. The significant incorporation of oxygen atoms onto the surface of PPT coated silica particles was further validated by Washburn capillary rise data, which demonstrated a substantial improvement of surface hydrophilicity. Plasma treatments conducted at low plasma specific energies of 0.15 to 0.3 kJ.cm^{-3} resulted in the maximum incorporation of oxygen atoms, where the influence of the ablation process was minimal. Water

plasma was found to be more efficient than air plasma for the treatment of PPT coated particles. Air plasma treated samples demonstrated lower negative zeta potentials and higher isoelectric points due to the presence of nitrogen-containing species on the surface. The greater surface area of silica particles compared to that of planar substrates resulted in relatively lower concentrations of –SOx(H) functionalities achieved on surfaces. Our introduced approach is greener, faster and simpler in comparison to previously reported wet-chemistry methods. This novel substrate-independent approach is applicable for the functionalization of almost any other particulate materials regardless of their shape and surface chemistry. The developed $–SO_x(H)$-functionalized particles could be applied in a wide range of applications such as biodiesel synthesis and water purification.

ACKNOWLEDGMENTS

The authors gratefully acknowledge the financial support of Government of South Australia, through the Premier Science and Research Fund (PSRF), National Centre of Excellence in Desalination Australia (NCEDA). The authors acknowledge the facilities, and scientific and technical assistance of the Australian Microscopy & Microanalysis Research Facility at the South Australian Regional Facility (SARF), University of South Australia, a facility that is funded by the University, and State and Federal Governments. We are thankful to Dr. John Denman for undertaking ToF-SIMS analysis.

REFERENCES

1. E. Andrijanto, E. A. Dawson and D. R. Brown, *Appl. Catal. B-Environ.*, 2012, **115**, 261-268.
2. P. Salek, L. Korecka, D. Horak, E. Petrovsky, J. Kovarova, R. Metelka, M. Cadkova and Z. Bilkova, *J. Mater. Chem.*, 2011, **21**, 14783-14792.
3. R. R. Guo and M. Y. Ding, *Colloid Surf. A-Physicochem. Eng. Asp.*, 2007, **292**, 153-158.
4. X. J. Deng, P. Yao, G. S. Ding and K. Lin, *Sci. Adv. Mater.*, 2013, **5**, 1032-1040.
5. S. J. Li, J. Hu and B. L. Liu, *J. Chem. Technol. Biotechnol.*, 2005, **80**, 531-536.
6. S. H. Zhang, J. Zhang and C. Horvath, *J. Chromatogr. A*, 2002, **965**, 83-92.
7. P. J. Majewski and T. M. Fuchs, *Adv. Powder Technol.*, 2007, **18**, 303-310.

8. Q. S. Qu, Q. Gu, Z. L. Gu, Y. Q. Shen, C. Y. Wang and X. Y. Hu, *Colloid Surf. A-Physicochem. Eng. Asp.*, 2012, **415**, 41-46.
9. M. Rat-Valdambrini, K. Belkacemi and S. Hamoudi, *Can. J. Chem. Eng.*, 2012, **90**, 18-25.
10. D. Kaner, A. Sarac and B. F. Senkal, *Environ. Geochem. Health*, 2010, **32**, 321-325.
11. D. V. Quang, J. E. Lee, J. K. Kim, Y. N. Kim, G. N. Shao and H. T. Kim, *Powder Technol.*, 2013, **235**, 221-227.
12. I. J. Dijs, H. L. F. van Ochten, C. A. van Walree, J. W. Geus and L. W. Jenneskens, *J. Mol. Catal. A: Chem.*, 2002, **188**, 209-224.
13. P. F. Siril, N. R. Shiju, D. R. Brown and K. Wilson, *Appl. Catal. A-Gen.*, 2009, **364**, 95-100.
14. M. Abdollahi, M. Rouhani, M. Hemmati and P. Salarizadeh, *Polym. Int.*, 2013, **62**, 713-720.
15. J. H. Seo, D. S. Shin, P. Mukundan and A. Revzin, *Colloid Surf. B-Biointerfaces*, 2012, **98**, 1-6.
16. C. L. Chen, A. Ogino, X. K. Wang and M. Nagatsu, *Diam. Relat. Mat.*, 2011, **20**, 153-156.
17. N. A. Bullett, J. D. Whittle, R. D. Short and C. W. I. Douglas, *J. Mater. Chem.*, 2003, **13**, 1546-1553.
18. M. S. Silverstein and I. Visoly-Fisher, *Polymer*, 2002, **43**, 11-20.
19. N. Vandencasteele and F. Reniers, *J. Electron Spectrosc. Relat. Phenom.*, 2010, **178-179**, 394-408.
20. K. L. Jarvis and P. Majewski, *J. Colloid Interface Sci.*, 2012, **380**, 150-158.
21. H. J. Griesser, K. S. Siow, L. Britcher and S. Kumar, *Plasma Processes Polym.*, 2006, **3**, 392-418.
22. S. R. Peri, H. Kim, B. Akgun, J. Enlow, H. Jiang, T. J. Bunning, X. F. Li and M. D. Foster, *Polymer*, 2010, **51**, 3971-3977.
23. B. Akhavan, K. Jarvis and P. Majewski, *Plasma Process. Polym.*, 2013, **10**, 1018-1029.
24. C. D. Easton, M. V. Jacob and R. A. Shanks, *Polymer*, 2009, **50**, 3465-3469.
25. R. Bogdanowicz, M. Sawczak, P. Niedziakowski, P. Zieba, B. Finke, J. Ryl, J. Karczewski and T. Ossowski, *J. Phys. Chem. C*, 2014, **118**, 8014-8025.
26. P. Rivolo, S. M. Severino, S. Ricciardi, F. Frascella and F. Geobaldo, *J. Colloid Interface Sci.*, 2014, **416**, 73-80.
27. K. S. Siow, L. Britcher, S. Kumar and H. J. Griesser, *Plasma Processes Polym.*, 2009, **6**, 583-592.
28. N. Inagaki, S. Tasaka and H. Miyazaki, *J. Appl. Polym. Sci.*, 1989, **38**, 1829-1838.
29. N. Inagaki, S. Tasaka and Z. Chengfei, *Polym. Bull.*, 1991, **26**, 187-191.
30. L. A. Komarnisky, R. J. Christopherson and T. K. Basu, *Nutrition*, 2003, **19**, 54-61.
31. B. Akhavan, K. Jarvis and P. Majewski, *Langmuir*, 2014, **30**, 1444-1454.
32. J. W. Kim and H. S. Choi, *J. Appl. Polym. Sci.*, 2002, **83**, 2921-2929.
33. M. Karches and P. R. von Rohr, *Surf. Coat. Technol.*, 2001, **142–144**, 28-33.

34. Y. Murata and T. Aradachi, *J. Electrost.*, 2001, **51**, 97-104.
35. N. De Vietro, R. d'Agostino and F. Fracassi, *Plasma Processes Polym.*, 2012, **9**, 911-918.
36. B. Akhavan, K. Jarvis and P. Majewski, *ACS Appl. Mater. Interfaces*, 2013, **5**, 8563-8571.
37. B. Akhavan, K. Jarvis and P. Majewski, *Powder Technol.*, 2013, **249**, 403-411.
38. K. L. Jarvis and P. Majewski, *Plasma Process. Polym.*, 2013, **10**, 619-626.
39. R. Zangi and B. J. Berne, *J. Phys. Chem. B*, 2006, **110**, 22736-22741.
40. S. Chander, R. Hogg and D. W. Fuerstenau, *Kona Powders Particles*, 2007, **25**, 56-75.
41. G. Le Dû, N. Celini, F. Bergaya and F. Poncin-Epaillard, *Surf. Coat. Technol.*, 2006, **201**, 5815-5821.
42. N. Moreau, O. Feron, B. Gallez, B. Masereel, C. Michiels, T. V. Borght, F. Rossi and S. Lucas, *Surf. Coat. Technol.*, 2011, **205**, S462-S465.
43. P. Hamerli, T. Weigel, T. Groth and D. Paul, *Surf. Coat. Technol.*, 2003, **174**, 574-578.
44. J. C. Vickerman and D. Briggs, *ToF-SIMS: Surface analysis by mass spectrometry*, Surfaces Spectra, Manchester, 2001.
45. D. Hegemann, E. Körner and S. Guimond, *Plasma Processes Polym.*, 2009, **6**, 246-254.
46. S. Hussain, R. Amade, E. Jover and E. Bertran, *Nanotechnology*, 2012, **23**.
47. J. Chai, F. Lu, B. Li and D. Y. Kwok, *Langmuir*, 2004, **20**, 10919-10927.
48. H. Y. Wang, T. Lu, F. H. Meng, H. Q. Zhu and X. Y. Liu, *Colloid Surf. B-Biointerfaces*, 2014, **117**, 89-97.
49. D. Hegemann, E. Körner, K. Albrecht, U. Schütz and S. Guimond, *Plasma Processes Polym.*, 2010, **7**, 889-898.
50. E. Moore, *Molecular modelling and bonding*, Royal Society of Chemistry, Cambridge, UK, 2002.
51. X. Crispin, S. Marciniak, W. Osikowicz, G. Zotti, A. W. D. Van der Gon, F. Louwet, M. Fahlman, L. Groenendaal, F. De Schryver and W. R. Salaneck, *J. Polym. Sci. Pt. B-Polym. Phys.*, 2003, **41**, 2561-2583.
52. A. Hollander and S. Kropke, *Plasma Processes Polym.*, 2010, **7**, 390-402.
53. O. Cavalleri, L. Oliveri, A. Dacca, R. Parodi and R. Rolandi, *Appl. Surf. Sci.*, 2001, **175**, 357-362.
54. S. Shylesh, S. Sharma, S. P. Mirajkar and A. P. Singh, *J. Mol. Catal. A: Chem.*, 2004, **212**, 219-228.
55. S. Y. Lee, C. Y. Ahn, J. Lee, J. H. Lee and J. H. Chang, *Nanoscale Res. Lett.*, 2012, **7**.
56. C. D. Bain and G. M. Whitesides, *J. Am. Chem. Soc.*, 1988, **110**, 5897-5898.
57. P. Majewski, *Int. J. Mater. Res.*, 2006, **97**, 784-788.
58. Y. Y. Ge, Z. L. Li, Y. X. Pang and X. Q. Qiu, *Int. J. Biol. Macromol.*, 2013, **52**, 300-304.
59. T. Jimbo, M. Higa, N. Minoura and A. Tanioka, *Macromolecules*, 1998, **31**, 1277-1284.
60. J. Kim and D. F. Lawler, *Bull. Korean Chem. Soc.*, 2005, **26**, 1083-1089.

61. S. H. Behrens and D. G. Grier, *J. Chem. Phys.*, 2001, **115**, 6716-6721.